J. Fluid Mech. (1992), *vol.* 238, *pp.* 55–71
Printed in Great Britain

Near-wall response in turbulent shear flows subjected to imposed unsteadiness

By REDA R. MANKBADI[1] AND JOSEPH T. C. LIU[2]†
[1]NASA Lewis Research Center, Cleveland, Ohio 44135
[2]Division of Engineering, Brown University, Providence, Rhode Island 02912

(Received 12 February 1991 and in revised form 12 September 1991)

Rapid-distortion theory is adapted to introduce a truly unsteady closure into a simple phenomenological turbulence model in order to describe the unsteady response of a turbulent wall layer exposed to a temporarily oscillating pressure gradient. The closure model is built by taking the ratio of turbulent shear stress to turbulent kinetic energy to be a function of the effective strain. The latter accounts for the history of the flow. The computed unsteady velocity fluctuations and modulated turbulent stresses compare favourably in the 'non-quasi-steady' frequency range, where quasi-steady assumptions would fail. This suggests that the concept of rapid distortion is especially appropriate for unsteady flows. This paper forms the basis for acoustical studies of the problem to be reported elsewhere.

1. Introduction

The study of unsteady turbulent flows is relevant in many technical applications, such as turbomachinery, Stirling engines, and nozzles. Pulsating turbulent flow in pipes and channels and over flat plates has received special attention recently because it provides relatively simple configurations for fundamental studies of unsteady turbulent shear flows and their possible control through forcing. Karlsson (1959) was the first to study pulsating turbulent boundary layers over a flat plate. More recently Binder & Kueny (1981), Cousteix, Houdeville & Janvelle (1981), Parikh, Reynolds & Jayaraman (1982), Binder *et al.* (1985), and Tardu, Binder & Blackwelder (1992) have experimentally studied pulsating flows in channels. Tu & Ramaprian (1983), Shemer & Wygnanski (1981), Shemer & Kit (1984), and Shemer, Wygnanski & Kit (1985) have addressed the pipe flow problem. A thorough review and compilation of existing data on pulsating, wall-bounded flows can be found in Carr (1981).

One general result from the experiments is that no preferred frequencies were found, in contrast to excited free turbulent flows. However, for wall-bounded flows the modification of the turbulence structure by pulsations nevertheless does depend on the frequency range. Carr (1981) pointed out that at low frequencies a quasi-steady behaviour is observed, as would be expected. The time- or Reynolds-averaged mean-flow velocity profile is practically the same as that for steady flow with the same local external flow. In this case, although there are significant variations in the turbulence energy and shear stress, their ratio remains at the quasi-steady value. As the imposed oscillation frequency is increased beyond a 'critical' value, significant interactions occur between the periodic oscillations and the turbulence structure. Mizushina, Maruyama & Shiozaki (1973) related this critical frequency to the

† Also CNRS, Laboratoire d'Aerothermique, F-92190 Meudon, France.

turbulent burst in the flow and showed that the turbulence intensity no longer follows that observed in the unperturbed-flow case. In the same postcritical frequency range Ramaprian, Tu & Menendez (1983), Binder *et al.* (1985), Mao & Hanratty (1986), and Tardu *et al.* (1992) also observed that the turbulence structure near the wall is perturbed out of equilibrium. The appropriately phased-averaged turbulence intensities and shear stress experience rather large frequency-dependent phase shifts.

Several attempts have recently been made at computing periodic turbulent shear flows at various levels of modelling effort (e.g. Cousteix *et al.* 1981; Tu & Ramaprian 1983; Menendez & Ramaprian 1983; Hanjalic & Stosic 1983; Cook, Murphy & Owen 1985; Mankbadi & Mobark 1991. The main defect is that these closure relations were identical to those used for steady flows and thus have not been successful, except in the quasi-steady region, in predicting results consistent with observations beyond the 'critical' frequency region, as pointed out by Hanjalic & Stosic (1983). Furthermore in these models the near-wall velocity was taken to be that given by the law of the wall for steady flows. Thus the important issue of the turbulent Stokes layer was completely circumvented. More recently Kebede *et al.* (1985), using the full Reynolds stress model but with quasi-steady closure, computed periodic turbulent flow properties down into the viscous layer region. For application to pulsating turbulent flows, however, the results were time-step dependent and deviated considerably from observations.

On the basis of their observations Binder & Kueny (1981) and Tardu *et al.* (1992) point out that the relevant dimensionless parameter of the near-wall region is the ratio of the viscous Stokes-layer lengthscale $(2\nu/\omega)^{\frac{1}{2}}$ to the near-wall viscous-layer lengthscale in turbulent shear flows ν/U_*, where ν is the kinematic viscosity, ω the forcing frequency, and U_* the frictional velocity. In fact the 'critical' frequency is in the range where the ratio of the two layers is of order unity. The so-called critical frequency region is now understood in terms of the parameter $l_s^+ = (2U_*^2/\nu\omega)^{\frac{1}{2}}$ being about 10. In this parameter region the dynamical effects of the periodic forcing strongly influence the wall-region viscous layer of the turbulent shear flow. In fact Cousteix (1986) concluded that a correct description of the near-wall region would be essential for obtaining the wall shear stresses in the intermediate- and high-frequency regions.

In the present paper we focus our attention on an appropriate, but simplified, modelling of pulsating turbulent flows in the 'high frequency' region in terms of the parameter l_s^+, where quasi-steady models have been known to be inadequate. The theoretical consideration naturally follows the feasibility indicated by Shemer & Kit's (1984) observations and by Gibson (1985) in separating the time-dependent, phase-averaged field from the time-independent, Reynolds-averaged field. In fact Carr's (1981) survey indicates that experimentally the mean field is not affected by the pulsations and can in fact be obtained from quasi-steady models. Therefore, we shall regard the mean flow as being given here. For the near-wall, phased-averaged field we shall solve the momentum equation for the periodic velocity component in conjunction with the phase-averaged turbulent kinetic energy equation supplemented with relations obtained from extensions of the rapid-distortion theory (e.g. Hunt & Carruthers 1990).

2. Formulation

The physical problem concerns the near-wall responses of periodically forced channel, pipe, or turbulent boundary-layer flow. To fix ideas, consider the flat-plate problem with an external velocity of the form

$$U_0(t) = \bar{U}_0 + \tilde{U}_0, \tag{1}$$

where t is the time, $\bar{U}_0$ is the time-averaged external velocity, $\tilde{U}_0 = A\exp(\mathrm{i}\omega t)$ is the imposed pulsation, and A is its amplitude. In the external region the oscillating velocity is equivalent to the oscillations in the pressure gradient given by the inviscid relation

$$\tilde{p}_x = -\mathrm{i}\omega A\exp(\mathrm{i}\omega t), \tag{2}$$

where $\tilde{p}$ is the oscillating pressure (with the fluid density absorbed into its denominator for convenience) and x is the streamwise coordinate. Differentiations are indicated by subscripts. Correspondingly the derivation of the fundamental equations for the mean motion, the periodic component, and the turbulence follows from the splitting of the total flow quantity $Q(x_i,t)$ into the three components:

$$Q(x_i,t) = \bar{Q}(x_i) + \tilde{q}(x_i,t) + q'(x_i,t), \tag{3}$$

where $\bar{Q}$ is the time-averaged component, $\tilde{q}$ the periodic component, and q' the turbulence. The derivation of the appropriate conservation equations is now fairly standard, even for multiply-interacting periodic modes (see e.g. Liu 1988, 1989). It suffices only to briefly outline the procedure and state the results of the simplified level. The time average, denoted by an overbar, is supplemented by the phase average, denoted by $\langle\ \rangle$. If we substitute the decomposition into the full Navier–Stokes equations for an incompressible fluid, the mean-flow momentum equations are obtained by time averaging. If we subtract the mean-flow equations from the phase-averaged ones, the momentum equations of the periodic component $\tilde{q}$ would be obtained. The crucial link with the turbulence comes from the modulated turbulent stresses denoted by

$$\tilde{r}_{ij} = \langle u_i' u_j' \rangle - \overline{u_i' u_j'}, \tag{4}$$

where u_j' denotes the turbulent velocity components.

The momentum equations for the turbulence are then obtained by subtracting the phase-averaged momentum equations from those for the total flow quantity. The definition of the modulated stresses $\tilde{r}_{ij}$ in (4) gives a clue to their derivation: the modulated turbulent kinetic energy, denoted by $\tilde{K}$, is but a special case of $\tilde{r}_{ij}$; its transport equation can also be obtained in a direct manner. The equations so obtained are stated in Liu (1988), and in the following we shall deal with limited versions, through appropriate arguments, for the physical problem at hand.

2.1. *Simplifications*

The extent of the near-wall region normal to the surface is 'thin' relative to the streamwise extent, and all x-derivatives (except for the external pressure) are neglected relative to the derivatives normal to the wall. The pressure is constant across the near-wall region. The vertical velocity is absent and the flow is unidirectional and thus $\tilde{u} = \tilde{u}(y,t)$, where y is the coordinate normal to the wall. The problem is further simplified by considering small perturbations, and a linear description suffices.

Even in this much-simplified framework, $\tilde{u}$ is coupled to the modulated and mean turbulent flow fields through the action of the modulated stress $\tilde{r}_{xy}$ in the $\tilde{u}$

momentum equation. Rather than dealing with transport equations for the shear and normal stresses, we chose to include only the modulated turbulent kinetic energy equation for $\tilde{K}$. This choice was motivated by the earlier work of Bradshaw, Ferriss & Atwell (1967) for the mean-flow problem. In this case there is no explicit need to make closure statements about the elusive pressure–velocity strain correlations because, for the energy equation, the action of the pressure gradients is recast into the 'diffusional' effect due to pressure work. If nonlinear effects are included, the diffusional effects would then also include the turbulent transport of $\tilde{K}$. This, together with the transport due to pressure work, can be neglected in the near-wall region in favour of viscous diffusion alone.

The simplified momentum equation for the periodic flow and the modulated turbulent energy equation are then, respectively,

$$\frac{\partial \tilde{u}}{\partial t} = -\frac{\partial \tilde{p}}{\partial x} + \nu \frac{\partial^2 \tilde{u}}{\partial y^2} - \frac{\partial \tilde{r}_{xy}}{\partial y}, \tag{5}$$

$$\frac{\partial \tilde{K}}{\partial t} = -\tilde{r}_{xy} \frac{\mathrm{d}\bar{U}}{\mathrm{d}y} - \bar{R}_{xy} \frac{\partial \tilde{u}}{\partial y} + \nu \frac{\partial^2 \tilde{K}}{\partial y_2} - \tilde{\epsilon}, \tag{6}$$

where $\bar{R}_{xy}$ is the mean Reynolds shear stress, which, together with the mean velocity $\bar{U}$, is considered as a given function of y. The problem requires the closure relation for the modulated viscous dissipation rate $\tilde{\epsilon}$ and the relation between $\tilde{r}_{xy}$ and $\tilde{K}$. The boundary conditions require the no-slip condition at the wall and that $\tilde{u}$ and $\tilde{K}$ approach some limit 'far' away from the wall. We shall state the boundary conditions after appropriate scaling, following closure arguments.

2.2. *Closure arguments: extensions of rapid-distortion ideas*

We refer to Hunt (1978), Hunt & Maxey (1978), and Hunt & Carruthers (1990) for a review of rapid-distortion theory and some of its applications and to Maxey (1982) for a re-examination of the theory with respect to descriptions of channel and pipe flows. The main formal assumption is that the fluctuating strain rates of the relatively large eddies are much weaker than the distortion due to the mean shear. For the perturbed 'high'-frequency turbulent shear flows it is conceivable that distortion would take place over timescales that are short relative to the timescales for the decay of the relatively large eddies. In this situation rapid-distortion theory could be justified for applications to the frequency range of practical interest.

On the other hand, for unperturbed turbulent shear flows, where the basic assumption of rapid distortion is not entirely satisfied, Townsend (1970, 1976) nevertheless has shown that the turbulence structure can be satisfactorily described. Although rapid-distortion theory does not provide the practical framework for a turbulent model, it does provide the ratio of the stresses to the turbulent kinetic energy in terms of an effective distortion strain. The quantitative formulation of the effective distortion strain then provides the remaining closure relation between the stresses and the energy. The extensions of these ideas to periodically perturbed turbulent shear flows are described here.

On the basis of an initial axisymmetric, rather than isotropic, spectrum tensor, Maxey (1982) computed velocity moments from the rapid-distortion theory that relate the general two-point velocity to such a tensor. The result for the ratio of the shear stress to the energy appears in the form

$$-R_{xy} = F(\alpha) K, \tag{7}$$

where R_{xy} is the shear stress, K is the kinetic energy, and α is taken to be the effective strain for a locally uniform shear; over an appropriate timescale α becomes a rate of strain. The function $F(\alpha)$ for small strains is of the form

$$F(\alpha) = \frac{a\alpha}{1+b\alpha^2}, \tag{8}$$

where $a = \frac{2}{5}[(3/S-1)/(1+2/S)]$ and $b = \frac{1}{35}[(21/S-15)/(1+2/S)]$. The initial anisotropy ratio S for shear flows is defined as the ratio of twice the largest normal stress (the streamwise component) to the sum of the two remaining normal stresses, evaluated at the centreline for pipe and channel flows. Maxey (1982) showed that existing experiments give S of about 1.8 for channel flows. The approximation of $F(\alpha)$ by (8) is correct to 10% over the range $0 < \alpha < 8$ (see Hunt & Maxey 1978, p. 255, and Maxey 1978). Since the maximum of α is 3.5 (Maxey 1982), this approximation should be within reasonable error. For locally uniform shear a relaxation equation describing the effective strain α was proposed by Maxey (1982) that in the present context takes the form

$$\frac{\partial\alpha}{\partial t} = \frac{\partial U}{\partial y} - \frac{\alpha}{T}, \tag{9a}$$

where T is an eddy timescale.

As Hunt (1978) pointed out, the advantage of (9*a*) is that it recovers the limit of equilibrium flow for long timescales, in which case

$$\alpha = T\frac{\mathrm{d}U}{\mathrm{d}y}, \tag{9b}$$

and for small timescales the rapid-distortion form is obtained:

$$\frac{\mathrm{d}\alpha}{\mathrm{d}t} = \frac{\mathrm{d}U}{\mathrm{d}y} \tag{9c}$$

The relation (9*b*) is used by Maxey (1982) to estimate the timescale T as follows. He analysed some experimental data to evaluate the stress ratios as a function of position. He then used distribution of the ratio $\tau/\rho u^2$ to specify a profile of effective strain by comparison with predicted results of rapid-distortion theory. Maxey found the profiles of the effective strain to be similar for most of the experiments considered, varying roughly linearly from zero to a maximum of about 3.5 at the wall. The ratio of mean shear to effective strain, (9*b*), gives an estimate of the distortion timescale T (see Maxey 1982, Table I, p. 274). The same procedure was followed herein, given $\mathrm{d}u/\mathrm{d}y$ at the wall and a maximum of 3.5 for the effective strain at the wall; T was calculated from (9*b*).

The imposed periodicity upon an existing steady external velocity, given by (1), then suggests the perturbation of (7)–(9), consistent with (5) and (6), in the following form:

$$R_{xy} = \bar{R}_{xy} + \tilde{r}_{xy}, \quad K = \bar{K} + \tilde{K},$$
$$F(\alpha) = F(\bar{\alpha}) + \tilde{\alpha}F'(\bar{\alpha}), \quad \alpha = \bar{\alpha} + \tilde{\alpha}, \quad U = \bar{U} + \tilde{u}, \tag{10}$$

where F' denotes the differentiation of F with respect to its arguments. Substituting (10) into (7)–(9) and linearizing gives the small-perturbation relations

$$-\tilde{r}_{xy} = F(\bar{\alpha})\tilde{K} + F'(\bar{\alpha})\bar{K}\tilde{\alpha}, \tag{11}$$

$$\frac{\partial\tilde{\alpha}}{\partial t} = \frac{\partial\tilde{u}}{\partial y} - \frac{\tilde{\alpha}}{T}. \tag{12}$$

Relations (11) and (12) will enable us to replace $\tilde{r}_{xy}$ by $\tilde{K}$ in (5) and (6).

The final closure argument is with regard to the modulated viscous dissipation rate $\tilde{\epsilon}$. We rely on the arguments that the small eddies contribute to viscous dissipation and that their timescales are such that they are nearly in equilibrium. In this case $\tilde{\epsilon}$ would be a perturbation from the usual postulated form (e.g. Alper & Liu 1978). For the present problem we shall deduce the form for $\tilde{\epsilon}$ directly from the perturbation energy equation (6). The argument for the smaller eddies is that there is a local equilibrium between production, given by the first two terms on the right-hand side of (6), and dissipation in the wall region (see e.g. Patel, Rodi & Scheuerer 1985). If we further hypothesize for estimating $\tilde{\epsilon}$ that an eddy viscosity relation might hold for both the mean and modulated stresses, and if the eddy viscosities are the same, then the two production terms are equal and are equated to the dissipation rate $\tilde{\epsilon} = -2\tilde{r}_{xy}\,\mathrm{d}\bar{U}/\mathrm{d}y$. Because of the local equilibrium arguments the quasi-steady form of the relation between stress and energy is used, leading finally to

$$\tilde{\epsilon} = 2F(\bar{\alpha})\frac{\mathrm{d}\bar{U}}{\mathrm{d}y}\tilde{K}. \tag{13}$$

Other simple models for $\tilde{\epsilon}$ (such as $\tilde{\epsilon} = \tilde{K}^{\frac{3}{2}}/\delta$) were considered, but no significant difference was found. It is believed that a modelled near-wall differntial equation for $\tilde{\epsilon}$ should be used to improve the dissipation model. As in the study of Patel *et al.* (1985), such an equation is known to be unreliable even for the high-Reynolds-number case (not including the wall layer). Therefore going to this complexity would complicate matters further and would confuse the main objective of this paper, which is to show that the rapid-distortion theory (and not an improved $\tilde{\epsilon}$ equation) can be used to account for truly non-steady effects in a turbulence model.

2.3. *Boundary-value problem: turbulent Stokes layer*

Subject to the driving external flow of the form (1), the perturbation flow quantities are also assumed to be harmonic and can be represented by the real part of

$$\tilde{q}(y,t) = \hat{q}(y)\exp(\mathrm{i}\omega t), \tag{14}$$

where the amplitude functions $\hat{q}(y)$ are complex. After substituting flow quantities of the form (14) into the system (5), (6), and (11)–(13), we further define non-dimensional quantities $U^+ = \bar{U}_0/U_*$, $R^+_{xy} = \bar{R}_{xy}/U_*^2$, $u^+ = \hat{u}/(A/U_*)$, $A^+ = A/U_*$, $K^+ = \hat{K}/A^+U_*^2$, $r^+_{xy} = \hat{r}_{xy}/A^+U_*^2$, $\omega^+ = \omega\nu/U_*^2$, $\epsilon^+ = \hat{\epsilon}\nu/A^+U_*^+$, $y^{++} = y^+/\omega^+$ and $y^+ = yU_*/\nu$. We recall that A is the amplitude of the periodic part of the external velocity and that $\bar{U}_0$ is its steady part, and in application to pipe or channel flow problems, these will be regarded as the centreline values. The dimensionless forms of (5) and (6) then appear as

$$\mathrm{i}\omega^+\hat{u}^+ = \mathrm{i}\omega^+ + (\hat{u}^+)'' - (\hat{r}^+_{xy})', \tag{15}$$

$$\mathrm{i}\omega^+\hat{K}^+ = -\hat{r}^+_{xy}(U^+)' - R^+_{xy}(\hat{u}^+)' + (K^+)'' - \hat{\epsilon}^+, \tag{16}$$

where a prime is used to denote differentiation with respect to y^+. Each of the terms in (15) and (16) has the same interpretation as the corresponding terms in (5) and (6). The boundary conditions are

$$y^{++} = 0, \quad \hat{u}^+ = \hat{K}^+ = 0 \tag{17a}$$

and

$$y^{++} \to \infty, \quad (\hat{u}^+)' = (\hat{K}^+)' = 0. \tag{17b}$$

The closure relations (11)–(13) become

$$-\hat{r}^+_{xy} = F(\bar{\alpha})\,\hat{K}^+ + \left(\frac{\mathrm{d}\ln F}{\mathrm{d}\bar{\alpha}}\right) R^+_{xy}\,\hat{\alpha}, \tag{18}$$

$$\hat{\alpha} = \frac{T^+(\hat{u}^+)'}{1+\mathrm{i}\omega^+ T^+}, \tag{19}$$

and

$$\hat{\epsilon}^+ = 2F(\bar{\alpha})\,(U^+)'\,\hat{K}^+, \tag{20}$$

where $T^+ = TU_*^2/\nu$. In (19) the representation (14) has also been applied to $\tilde{\alpha}$.

2.4. *Numerical problem*

The system of equations (15), (16), and (18)–(20) and the boundary conditions (17) form a boundary-value problem. The variable coefficients, such as R^+_{xy} and $(U^+)'$, were obtained from experimental data in the wall region (Laufer 1954; Schubauer 1954; Derksen & Azad 1981; El-Telbany & Reynolds 1981; Patel *et al.* 1985) and fitted with simple functions of y^+.

The boundary-value problem was then solved by using the SUPORT program (Scott & Watts 1975). The method of solution uses superposition coupled with an orthonormalization procedure and a variable-step Runge–Kutta–Fehlberg integration scheme. Each time the superposition solutions begin to lose their numerical linear independence, the vectors are reorthonormalized before integration proceeds. The basic principle of the algorithm is then to piece together the intermediate orthogonalized solutions, defined on the various subintervals, to obtain the desired solutions.

3. Results and discussion

We have previously defined the parameter l_s^+, which is essentially the ratio of the Stokes-layer thickness $(2\nu/\omega)^{\frac{1}{2}}$ to the near-wall-region viscous lengthscale ν/U_*. Now l_s^+ is related to the dimensionless frequency ω^+ as $l_s^+ = (2/\omega^+)^{\frac{1}{2}}$; when the viscous Stokes layer becomes of the same order as the wall-region viscous layer, $l_s^+ \approx 10$, in which case $\omega^+ \approx 0.02$. This is the range of the parameter ω^+ when strong unsteady interactions take place in the near-wall region.

3.1. *Phase-averaged streamwise velocity*

The calculated oscillations in the streamwise velocity are compared with the experimental data of Binder & Kueny (1981) and Binder *et al.* (1985) in figure 1. Figure 1(*a*) is for the case of $l_s^+ = 5.6$ ($\omega^+ = 0.0637$), and figure 1(*b*) for $l_s^+ = 17$ ($\omega^+ = 0.0069$). In the higher-frequency case an amplitude overshoot occurs, as would be expected of Stokes-like viscous layers, and this overshoot moves toward the wall as the frequency is increased. For the high- and low-frequency cases the amplitudes agree reasonably well with the data. The phase angle, relative to that of the imposed velocity oscillations, compares well with the data for the higher-frequency case. The phase shift near the wall is positive and approaches the Stokes value $\frac{1}{4}\pi$. In the lower-frequency case the agreement for the phase shift is less satisfactory.

3.2. *Phase-averaged wall shear stress*

The oscillating wall shear stress is shown in figure 2 in comparison with the measurements of Binder *et al.* (1985). The magnitude, normalized by the Stokes value at the same frequency, is given in figure 2(*a*). The derivation from unity represents

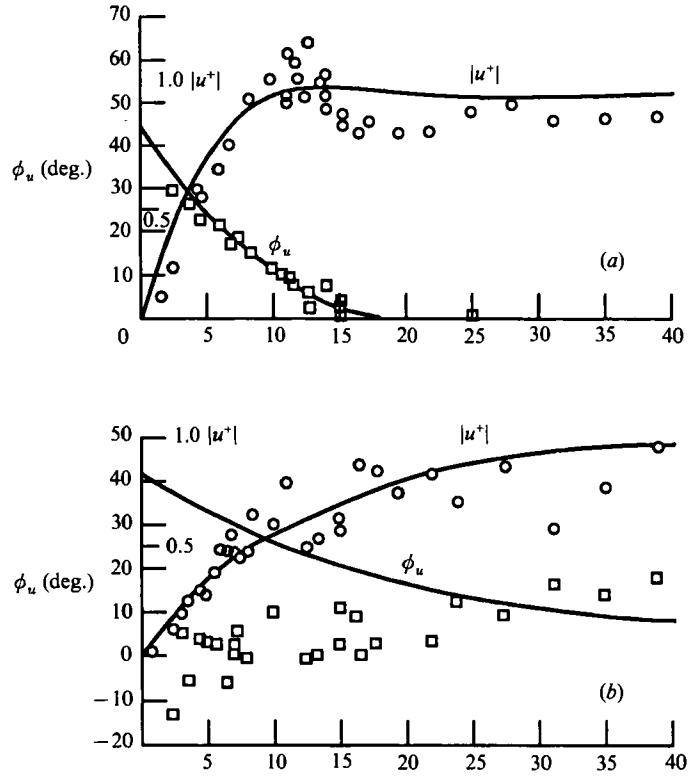

FIGURE 1. Computed phase-averaged streamwise velocity (curves) compared with data of Binder & Kueny (1981) and Binder *et al.* (1985) (symbols), in terms of magnitude of u^+ and phase angle ϕ_u relative to their respective imposed values. (*a*) $\omega^+ = 0.0637$ ($l_s^+ = 5.6$), (*b*) $\omega^+ = 0.0069$ ($l_s^+ = 17$).

the departure of the present solution from that of the laminar Stokes layer. The phase angle ϕ_τ, referenced to the phase of the free-stream velocity, is shown in figure 2(*b*). Although the present theory is concerned with the relatively 'high'-frequency region $l_s^+ \approx 10$ ($\omega^+ \approx 0.02$), the results are nevertheless shown for the extended region $l_s^+ \approx 70$ ($\omega^+ \approx 0.0004$), covering the low-frequency, quasi-steady region. The region of validity of the present theory can thus be examined. As expected, figure 2(*a*) shows that the computed amplitude of the wall shear stress is in good agreement with the data in the region $l_s^+ \lesssim 20$ ($\omega^+ > 0.005$). At these 'high' frequencies the wall shear stress amplitudes dip below the Stokes value, as in the experiments. This behaviour was first observed by Ronneberger & Ahrens (1977) and also by Parikh *et al.* (1982). At intermediate frequencies the modulated shear stress increases over the Stokes values as in the observations. At larger values of l_s^+ the wall shear stress magnitude is underestimated relative to observations.

The computed wall shear stress is also compared in figure 3 with the experimental data of Mao & Hanratty (1986) and Ramaprian & Tu (1983) as well as the predictions of the quasi-steady $K-\epsilon$ model (Mankbadi & Mobark 1991). The magnitude of the oscillatory wall shear stress is normalized by the mean wall shear stress and by the dimensionless forcing velocity (equivalent to the A defined previously). Mao & Hanratty's (1986) data are in the intermediate- to high-frequency range and therefore are more relevant to the present analysis. Figure 3(*a*) shows that the computed value is in good agreement with observations for $\omega^+ > 0.005$, as expected. For the $K-\epsilon$ model the agreement with experimental data in the low-frequency

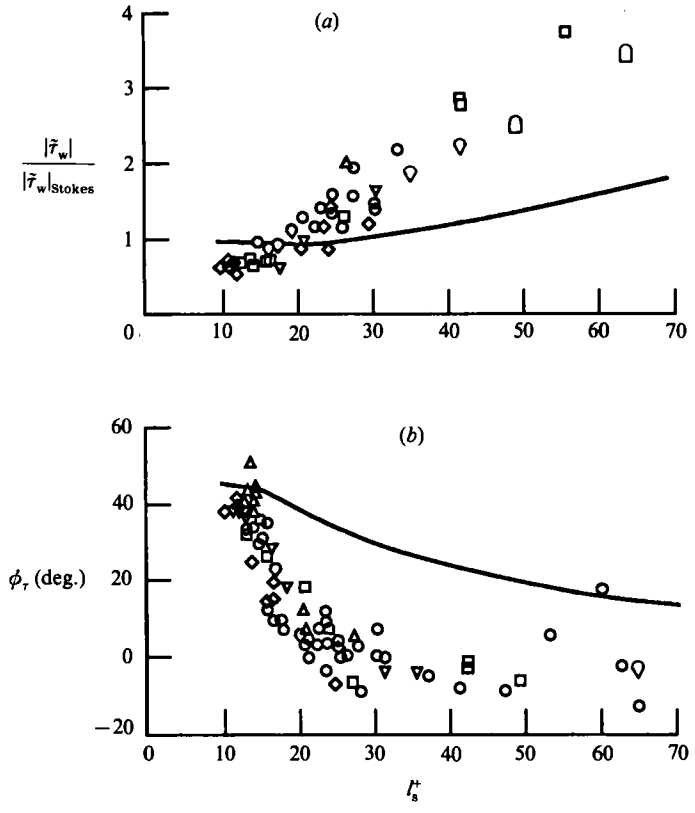

FIGURE 2. Computed wall shear stress compared with data of Binder *et al.* (1985), including forcing at large amplitudes: ○, $A/U_0 = 0.1$; □, 0.13; △, 0.17; ◇, 0.19; ▽, 0.27; ♀, 0.60; ⌂, 0.70. (*a*) Amplitude $|\tilde{\tau}_w|/|\tilde{\tau}_w|_{Stokes}$, (*b*) phase angle.

range is acceptable, but the figure clearly shows the failure of the $K-\epsilon$ model in the high-frequency range, where the present model becomes highly accurate. The phase angle in figure 3(*b*) behaves qualitatively as observations in the frequency region $\omega^+ > 0.015$. It approaches an asymptotic value of about $\frac{1}{4}\pi$. In the low-frequency region the phase angle is overestimated.

3.3. *Modulated turbulent kinetic energy*

The amplitude of the modulated turbulent kinetic energy K^+ is shown in figure 4 at several frequencies. The figure shows that the peak in the amplitude of the modulated turbulent kinetic energy moves closer to the wall with increasing frequency and it also decays rapidly with increasing frequency. Thus the thickness of the layer where turbulence is influenced by the imposed oscillations decreases with increasing frequency. The figure clearly indicates that the amplitude of the modulated turbulent kinetic energy decreases with increasing frequency. Thus the turbulence reaches a state of frozen structure at high frequencies.

The present predictions of frozen turbulence at high frequencies is consistent with several experimental observations, such as those of Parikh *et al.* (1982). Turbulence models based on quasi-steady assumptions in which the turbulent stresses are proportional to the instantaneous velocity gradient cannot predict such phenomena. The local time derivative of the velocity increases indefinitely, but the effective

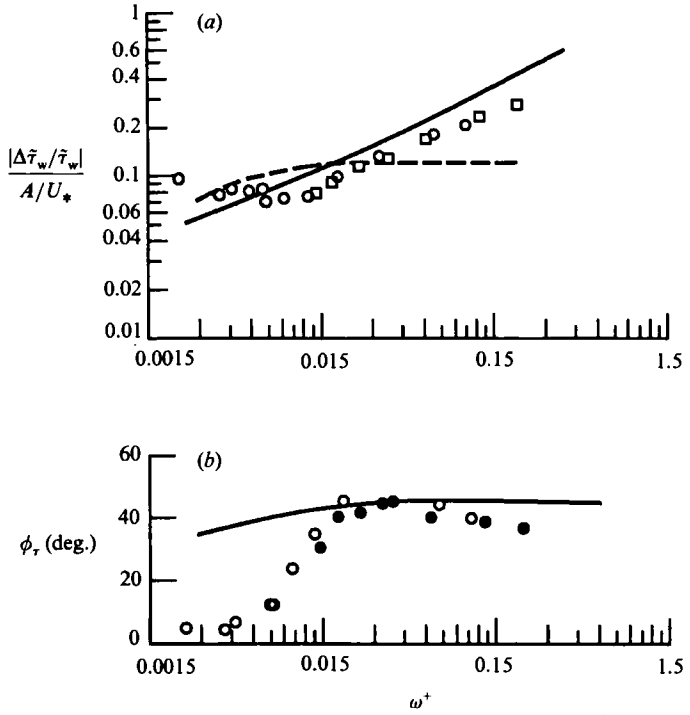

FIGURE 3. Computed phase-averaged wall shear stress compared with data of ○, ●, Mao & Hanratty (1986); and □, Ramaprian & Tu (1983). (*a*) Amplitude $(|\tilde{\tau}_w|/\bar{\tau}_w)/(A/U_*)$, (*b*) phase angle. In (*a*) the dashed line is from the quasi-steady $K-\epsilon$ model (Mankbadi & Mobark 1991).

strain reaches a finite value. As the frequency goes to infinity, the effective strain becomes zero. Therefore in the present model the turbulence can reach a state of frozen structure.

3.4. *Modulated normal stress*

We recall the definition of the modulated turbulent normal stress due to the streamwise component of the turbulence fluctuation, $\tilde{\tau}_{xx} = \langle (u')^2 \rangle - \overline{(u')^2}$. This quantity is of particular interest here in that it has been measured by Binder *et al.* (1985). The modulated stresses $\tilde{\tau}_{xx}$ are obtained here as a byproduct of the computation by relating them to the turbulent kinetic energy through a function of the strain rate similar to that of (8) (see Maxey 1978, 1982). A comparison between our computed results and experimental data is given in figure 5 for the two values of ω^+, 0.03 and 0.0038. The main features of the observed structure are obtained by the present theory. The peak values of $\tilde{\tau}_{xx}$ and its y^+ location both decrease slightly as ω^+ increases. In fact, the location of the peak is actually well described by the theory. However, figure 5 indicates that this component of the normal stress is underestimated by the theory. This might be due to the overestimation of the viscous dissipation rate near the wall.

The phase angle of the oscillations in the modulated turbulent normal stress, relative to that of the oscillations in the local axial velocity component, $\phi_{\tilde{\tau}_{xx}} - \phi_{\tilde{u}}$, is shown in figure 6 for several frequencies. The figure shows certain trends that are consistent with observations. The angle between $\tilde{\tau}_{xx}$ and $\tilde{u}$ increases with increasing frequency. The phase angle is negative, indicating a time lag that increases away from the wall, as observed by Ramaprian & Tu (1983). At high frequencies the peak in the magnitude of occurs at a phase lag of about 90° (i.e. during the deceleration

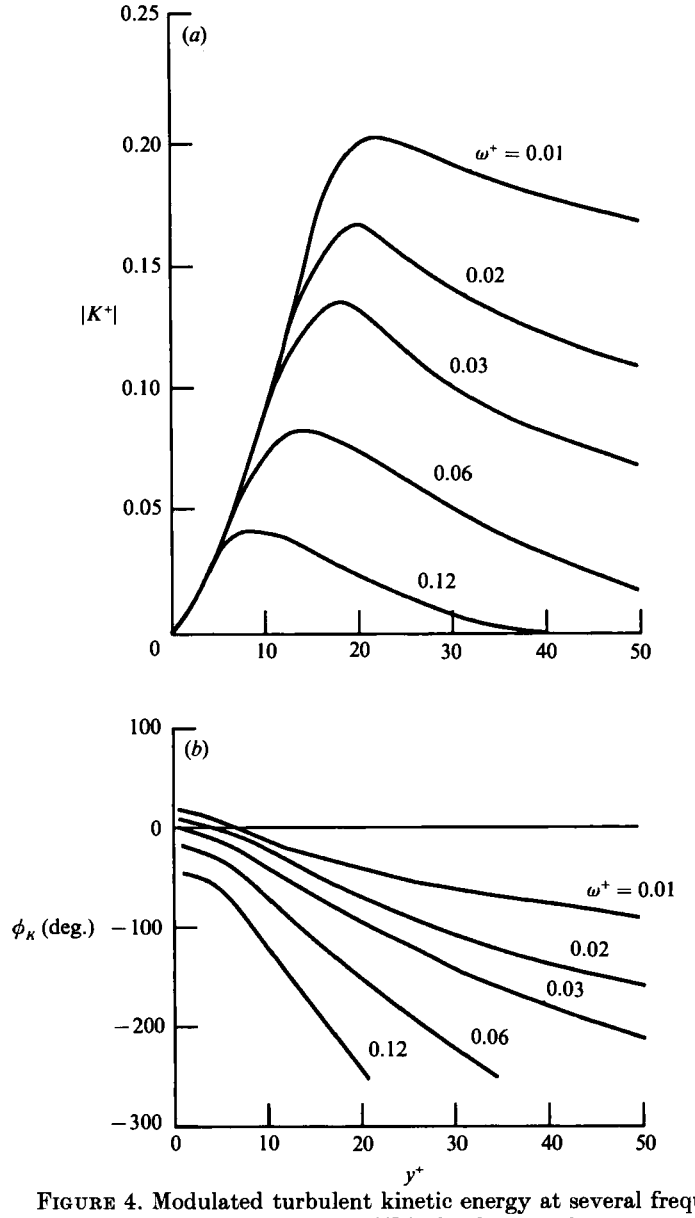

FIGURE 4. Modulated turbulent kinetic energy at several frequencies. (*a*) Amplitude $|K^+|$, (*b*) phase angle.

phase as described by Binder *et al.* 1985). The figure shows that the phase lag increases with increasing frequency and attains a minimum close to the wall ($1 < y^+ < 5$), as observed in the case of pulsating pipe flow by Shemer *et al.* (1985). Even at the lowest frequency shown, figure 6 illustrates that there is still a phase lag of $\tilde{r}_{xx}$ behind $\tilde{u}$, especially away from the wall. This is in accordance with Shemer & Kit's (1984) observations for quasi-steady turbulent pulsaing flow in a pipe. The phase distribution thus seems to be sensitive to deviation from quasi-steady assumptions. This is in accordance with investigations of Ramaprian *et al.* (1983), which clearly demonstrated that the turbulence structure cannot be associated with the corresponding oscillating velocity in a simple manner.

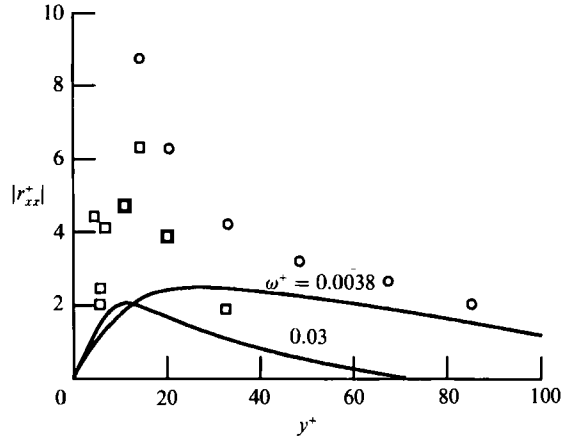

FIGURE 5. Magnitudes of modulated turbulent streamwise normal stress $|\tilde{r}_{xx}|$ compared with data of Binder *et al.* (1985): □, $\omega^+ = 0.03$; ○, $\omega^+ = 0.0038$.

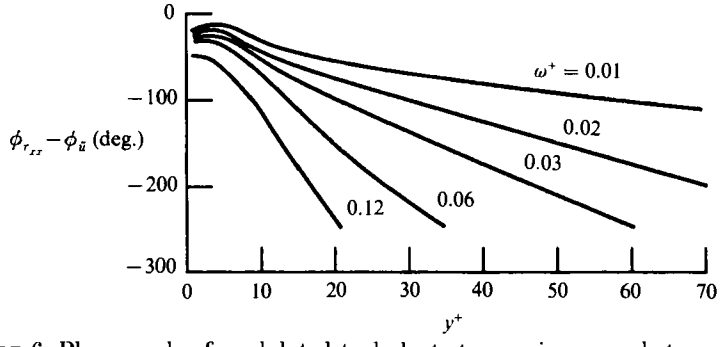

FIGURE 6. Phase angle of modulated turbulent streamwise normal stress r^+_{xx} (relative to phase angle of oscillating external flow).

3.5. *Modulated turbulent shear stress*

The calculated oscillations in the shear stress $\tilde{r}_{xy}$ are shown in figure 7 for several frequencies. The figure shows that the peak in the amplitude of oscillation decreases with increasing frequency and moves closer to the wall. This feature again indicates that the turbulence tends to reach a frozen state at high frequencies. To examine the relation between the oscillating turbulent shear stress and the oscillating velocity gradient, we show the latter in figure 8. By comparing figure 7(*a*) with figure 8(*a*), it can be seen that the Reynolds stress as a function of y^+ varies considerably less than the oscillating velocity gradient, especially at high frequencies.

3.6. *Departure from structural equilibrium*

To examine the departure of the flow from structural equilibrium, we examine the ratio of the modulated shear stress to the modulated turbulent energy $\tilde{r}_{xy}/\tilde{K}$. For equilibrium flows this ratio should be the same as that of the steady flow. The amplitude of this ratio is shown in figure 9(*a*). The figure shows that the departure from equilibrium increases with the frequency. This departure reaches a maximum near the wall ($3 < y^+ < 8$). For $y^+ > 20$ the flow behaves like a quasi-steady one. This is consistent with the structure of oscillating turbulent boundary layers observed by Ramaprian *et al.* (1983). Figure 9(*b*) shows that the phase angle of the modulated

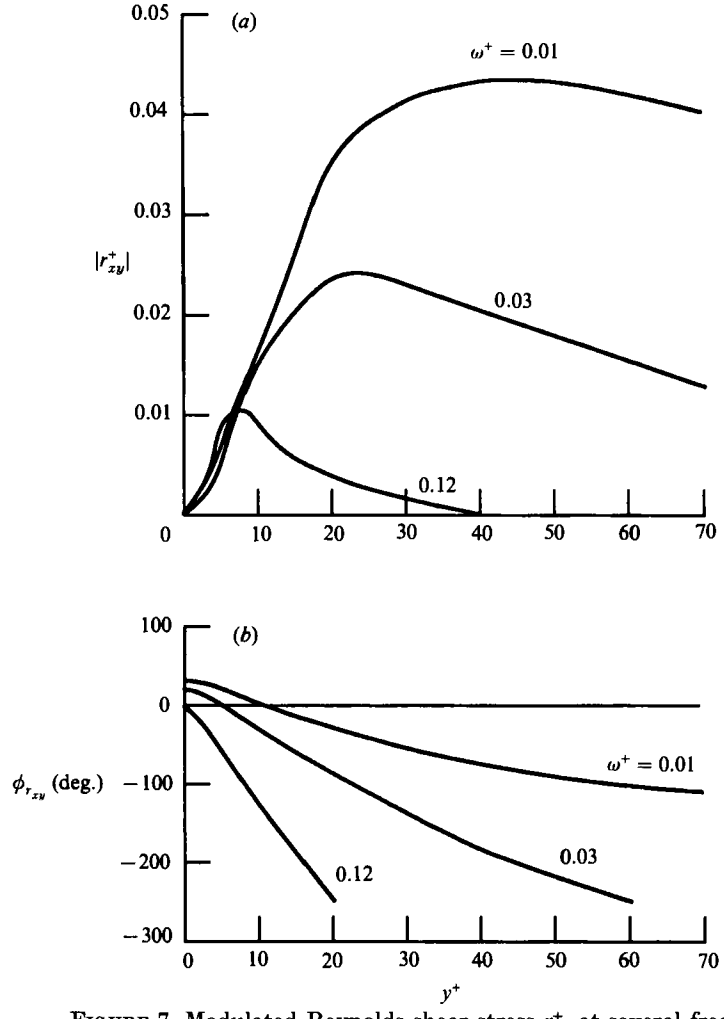

FIGURE 7. Modulated Reynolds shear stress r^+_{xy} at several frequencies. (*a*) Amplitude $|r^+_{xy}|$, (*b*) phase angle.

shear stress leads that of the energy and that this lead increases with the frequency. The phase lead is maximum near the wall and decrease rapidly away from the wall. These results, as well as previous experimental observations, emphasize that at intermediate- and high-frequency ranges of oscillation the turbulent kinetic energy and the Reynolds shear stress are mutually out of phase. Thus eddy viscosity models relating the turbulence properties to the instantaneous local mean flow cannot accurately predict such flows in the region near the wall.

The concept proposed by Shemer & Wygnanski (1981) of time-dependent eddy viscosity, which accounts for the memory of the turbulence incorporating a relaxation time, might be an improvement over the time-independent eddy viscosity models. However, the time-dependent eddy viscosity must necessarily be complex in order to include phase-lag effects. Some of these ideas were anticipated much earlier by Betchov & Criminale (1967, p. 255).

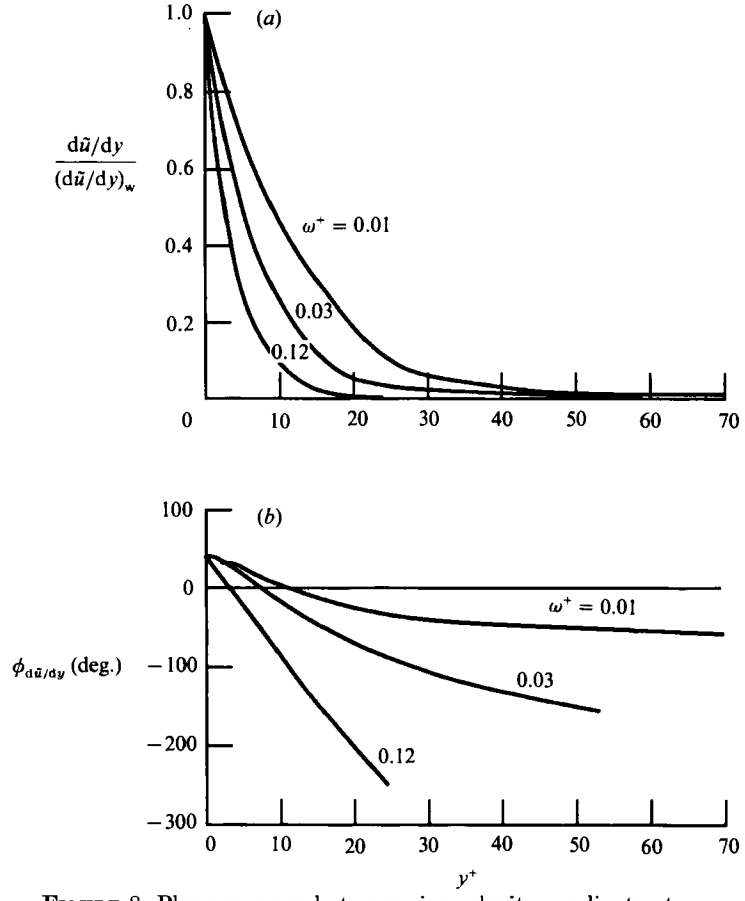

FIGURE 8. Phase-averaged streamwise velocity gradients at several frequencies. (*a*) Amplitude $(d\tilde{u}/dy)/(d\tilde{u}/dy)_w$, (*b*) phase angle.

4. Concluding remarks

The modulated turbulent kinetic energy and momentum equations were solved for the case of a boundary layer subjected to imposed oscillations in the external flow. The rapid-distortion theory was used to relate the modulated Reynolds shear stress to the modulated turbulent kinetic energy. Predicted results compared well with observations for frequencies larger than about $\omega^+ = 0.005$.

The results obtained for the intermediate- to high-frequency range showed several trends consistent with observations:

(i) At high frequencies the modulated wall shear stress decreases below the Stokes value. At intermediate frequencies it increases over the Stokes value.

(ii) At high frequencies the modulated wall shear stress leads the oscillation in the mean flow by about 45°. This phase lead decreases with decreasing frequency.

(iii) The peak of the amplitude of oscillations in the modulated kinetic energy decays rapidly with increasing frequency and moves closer to the wall. Turbulence tends to reach a state of frozen structure at high frequencies.

(iv) There are large phase differences between the oscillations in the turbulence and those in the mean flow. These phase differences increase with the frequency. Thus the near-wall turbulence cannot be modelled by relating it to the local instantaneous mean-flow parameters.

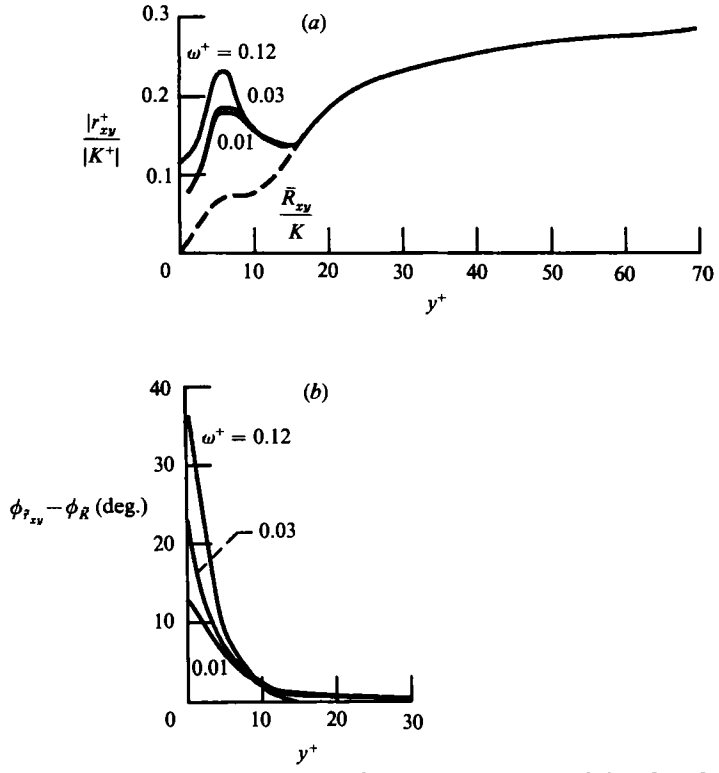

FIGURE 9. Ratio of modulated Reynolds shear stress to modulated turbulent kinetic energy. (*a*) Amplitude $|r^+_{xy}|/|K^+|$, (*b*) phase difference.

(v) The phase lag between the oscillations in the turbulence and the oscillations in the mean flow is minimum around $1 < y^+ < 5$, indicating that the turbulence is first produced near the wall.

Examining the ratio of the oscillations in the Reynolds shear stress to the oscillations in the turbulent kinetic energy indicates that the deviation from quasi-steady assumptions increases with the frequency. This deviation is restricted to a thin layer next to the wall. The phase angle is more sensitive than the amplitude to the deviation from quasi-steady assumptions.

The features obtained from the present theory are sufficiently encouraging that it seems worthwhile to develop ideas from rapid-distortion theory for further use in describing a class of unsteady turbulent shear flows, including the fascinating problems involving coherent structures and their control (Liu 1988, 1989; Mankbadi 1992).

The authors wish to acknowledge helpful discussions with M. Maxey. This work was supported by NASA Lewis Research Center, Grant NAG3-1016, the NSF Fluid Particulate and Hydraulic Systems Program, and DARPA/URI while monitored by Dr H. S. Wisniewski. J.T.C.L. acknowledges the hospitality of Laboratoire d'Aerothermique, CNRS/Meudon particularly that of Dr M.-F. Scibilia, and Ministere de la Recherche et de la Technologie.

REFERENCES

ALPER, A. & LIU, J. T. C. 1978 On the interactions between large-scale structure and fine-grained turbulence in a free shear flow. II. The development of the spatial interactions in the mean. *Proc. R. Soc. Lond.* A **359**, 497–523.

BETCHOV, R. & CRIMINALE, W. O. 1967 *Stability of Parallel Flows*. Academic.

BINDER, G. & KUENY, J. L. 1981 Measurements of the periodic velocity oscillations near the wall in unsteady turbulent channel flow. In *Unsteady Turbulent Shear Flows, IUTAM Symp.* (ed. R. Michel, J. Cousteix & R. Houdeville), pp. 100–109. Springer.

BINDER, G., TARDU, S., BLACKWELDER, R. F. & KUENY, J. L. 1985 Large amplitude periodic oscillations in the wall region of a turbulent channel flow. In *5th Symp. on Turbulent Shear Flows*, pp. 16.1–16.8. Pennsylvania State University Press.

BRADSHAW, P., FERRISS, D. H. & ATWELL, N. P. 1967 Calculation of boundary layer development using the turbulent energy equation. *J. Fluid Mech.* **28**, 593–616.

CARR, L. W. 1981 A review of unsteady boundary layer experiments. In *Unsteady Turbulent Shear Flows, IUTAM Symp.* (ed. R. Michel, J. Cousteix & R. Houdeville), pp. 3–35. Springer.

COOK, W. J., MURPHY, J. D. & OWEN, F. K. 1985 An experimental and computational study of turbulent boundary layers in oscillating flows. In *5th Symp. on Turbulent Shear Flows*, pp. 18.3–18.18. Pennsylvania State University Press.

COUSTEIX, J. 1986 Three-dimensional and unsteady boundary-layer computations. *Ann. Rev. Fluid Mech.* **18**, 173–196.

COUSTEIX, J., HOUDEVILLE, R. & JANVELLE, J. 1981 Response of a turbulent boundary layer to a pulsation of the external flow with and without adverse pressure gradient. In *Unsteady Turbulent Shear Flows, IUTAM Symp.* (ed. R. Michel, J. Cousteix & R. Houdeville), pp. 120–144. Springer.

DERKSEN, R. W. & AZAD, R. S. 1981 Behavior of the turbulent energy equation at a fixed boundary. *AIAAA J.* **19**, 238–239.

EL-TELBANY, M. M. M. & REYNOLDS, A. J. 1981 Turbulence in plane channel flows. *J. Fluid Mech.* **111**. 283–318.

GIBSON, M. M. 1985 Boundary layers. *In Turbulent Shear Flows 4*, (ed. L. J. S. Bradbury *et al.*), pp. 219–222. Springer.

HANJALIC, K. & STOSIC, N. 1983 Hysteresis of turbulent stresses in wall flows subjected to periodic disturbances. In *Turbulent Shear Flows 4*, (ed. L. J. S. Bradbury *et al.*), pp. 287–300. Springer.

HUNT, J. C. R. 1978 A review of the theory of rapidly distorted turbulent flows and its applications. *Fluid Dyn. Trans.* **9**, 121–152.

HUNT, J. C. R. & CARRUTHERS, D. J. 1990 Rapid distortion theory and the 'problems' of turbulence. *J. Fluid Mech.* **212**, 497–532.

HUNT, J. C. R. & MAXEY, M. R. 1978 Estimating velocities and shear stresses in turbulent flows of liquid metals driven by low frequency electromagnetic fields. In *MHD-Flows and Turbulence II* (ed. H. Branover), pp. 249–269. Israel University Press.

KARLSSON, S. K. F. 1959 An unsteady turbulent boundary layer. *J. Fluid Mech.* **5**, 622–636.

KEBEDE, W., LAUNDER, B. E. & YOUNIS, B. A. 1985 Large-amplitude periodic pipe flow: A second-moment closure study. In *5th Symp. on Turbulent Shear Flows 5*, pp. 16.23–16.29. Pennsylvania State University Press.

LAUFER, J. 1954 The structure of turbulence in fully developed pipe flow. *NACA Rep.* 1174.

LIU, J. T. C. 1988 Contributions to the understanding of large-scale coherent structures in developing free turbulent shear flows. *Adv. Appl. Mech.* **26**, 183–309.

LIU, J. T. C. 1989 Coherent structures in transitional and turbulent free shear flows. *Ann. Rev. Fluid Mech.* **21**, 285–315.

MANKBADI, R. R. 1992 Dynamics and control of coherent structures in turbulent jets. *Appl. Mech. Rev.* **45** (in press).

MANKBADI, R. R. & MOBARK, A. 1991 Quasi-steady turbulence modeling of unsteady flows. *J. Heat & Fluid Flow* **12**, 122–129.

MAO, Z-X. & HANRATTY, T. J. 1986 Studies of the wall shear stress in a turbulent pulsating pipe flow. *J. Fluid Mech.* **170**, 545–564.

MAXEY, M. R. 1978 Aspects of unsteady turbulent shear flow. Ph.D. dissertation, University of Cambridge.

MAXEY, M. R. 1982 Distortion of turbulence in flows with parallel streamlines. *J. Fluid Mech.* **124**, 261–282.

MENENDEZ, A. N. & RAMAPRIAN, B. R. 1983 Study of unsteady turbulent boundary layers. *Iowa Inst. Hydraul. Res. Rep.* 270. (Avail. NTIS, AD-A138156.)

MIZUSHINA, T., MARUYAMA, T. & SHIOZAKI, Y. 1973 Pulsating turbulent flow in a tube. *J. Chem. Engng Japan* **6**, 287–294.

PARIKH, P. G., REYNOLDS, W. C. & JAYARAMAN, R. 1982 Behavior of an unsteady turbulent boundary layer. *AIAA J.* **20**, 769–775.

PATEL, V. V., RODI, W. & SCHEUERER, G. 1985 Turbulence models for near-wall and low-Reynolds-number flows-A review. *AIAA J.* **23**, 1308–1319.

RAMAPRIAN, B. R. & TU, S. W. 1983 Fully developed periodic turbulent pipe flow. Part 2. The detailed structure of the flow. *J. Fluid Mech.* **137**, 59–81.

RAMAPRIAN, B. R., TU, S. W. & MENENDEZ, A. N. 1983 Periodic turbulent shear flows. *In Turbulent Shear Flows 4* (ed. L. J. S. Bradbury *et al.*), pp. 301–310. Springer.

RONNEBERGER, D. & AHRENS, C. D. 1977 Wall shear stress caused by small amplitude perturbations of turbulent boundary-layer flow: an experimental investigation. *J. Fluid Mech.* **83**, 433–464.

SCHUBAUER, G. B. 1954 Turbulent processes as observed in boundary layer and pipe. *J. Appl. Phys.* **25**, 188–196.

SCOTT, M. R. & WATTS, H. A. 1975 SUPORT – A computer code for two-point boundary value problems via orthonormalization. *Sandia Labs., Rep.* SAND-75-0198.

SHEMER, L. & KIT, E. 1984 An experimental investigation of the quasi-steady turbulent pulsating flow in a pipe. *Phys. Fluids* **27**, 72–76.

SHEMER, L. & WYGNANSKI, I. 1981 Pulsating flow in a pipe. In *Symp. on Turbulent Shear Flows 3*, pp. 8.13–8.18. Pennsylvania State University Press.

SHEMER, L., WYGNANSKI, I. & KIT, E. 1985 Pulsating flow in a pipe. *J. Fluid Mech.* **153**, 313–337.

TARDU, S. F., BINDER, G. & BLACKWELDER, R. F. 1992 Turbulent channel flow with large amplitude velocity oscillations. *J. Fluid Mech.* (submitted).

TOWNSEND, A. A. 1970 Entrainment and the structure of turbulent flow. *J. Fluid Mech.* **41**, 13–46.

TOWNSEND, A. A. 1976 *The Structure of Turbulent Shear Flow*, 2nd edn., pp. 80–88, 105–129. Cambridge University Press.

TOWNSEND, A. A. 1980 The response of sheared turbulence to additional distortion. *J. Fluid Mech.* **98**, 171–191.

TU, S. W. & RAMAPRIAN, B. R. 1983 Fully developed periodic turbulent pipe flow. Part 1. Main experimental results and comparison with predictions. *J. Fluid Mech.* **137**, 31–58.